Siderophile volatile element inventory in lunar magmatic rocks and mantle sources

Philipp Gleißner, Julie Salme, Harry Becker

Freie Universität Berlin, Institut für Geologische Wissenschaften, Malteserstr. 74-100, 12249 Berlin, Germany

Article history: Received 5 March 2022 Received in revised form 1 June 2022 Accepted 9 June 2022

Earth andPlanetaryScienceLetters593(2022)117680 https://doi.org/10.1016/j.epsl.2022.117680

Corresponding author: E-mail address: gleissner@zedat.fu-berlin.de

Abstract:

Elevated water contents in various lunar materials have invigorated the discussion on the volatile content of the lunar interior and on the extent to which the volatile element inventory of lunar magmatic rocks is controlled by volatility and degassing. Abundances of moderately volatile and siderophile elements can reveal insights into lunar processes such as core formation, late accretion and volatile depletion. However, previous assessments relied on incomplete data sets and data of variable quality. Here we report mass fractions of the siderophile volatile elements Cu, Se, Ag, S, Te, Cd, In, and Tl in lunar magmatic rocks, analyzed by state-of-the-art isotope dilution-inductively coupled plasma mass spectrometry. The new data enable us to disentangle distribution processes during the formation of different magmatic rock suites and to constrain mantle source compositions. Mass fractions of Cu, S, and Se in mare basalts and magnesian suite norites clearly correlate with indicators of fractional crystallization. Similar mass fractions and fractional crystallization trends in mafic volcanic and plutonic rocks indicate that the latter elements are less prone to degassing during magma ascent and effusion than proposed previously. The latter processes predominate only for specific elements (e.g., Tl, Cd) and complementary enrichments of these elements also occur in some brecciated highland rocks. A detailed comparison of elements with different affinities to metal or sulfide and gas phase reveals systematic differences between lunar magmatic rock suites. The latter observation suggests a predominant control of the variations of S, Se, Cu, and Ag by mantle source composition instead of late-stage magmatic degassing. New estimates of mantle source compositions of two low-Ti mare basalt suites support the notion of a lunar mantle that is strongly depleted in siderophile volatile elements compared to the terrestrial mantle.

Keywords: Lunar impactites; HSE; Late accretion

1. Introduction

The presence or absence of volatiles in the Moon has important consequences for our understanding of its formation and differentiation. Since the era of the Apollo missions, the Moon was thought to be highly depleted in volatile elements relative to Earth and chondrites. As inferred mainly from mass fractions of moderately and highly volatile elements in lunar basalts, estimates of the composition of the bulk lunar mantle define a significantly steeper volatile depletion curve than for Earth (Albarède et al., 2015; O'Neill, 1991). Stable isotope studies of moderately volatile elements such as Zn or K in lunar rocks have been interpreted to indicate that the volatile element depletion is most likely a direct or indirect consequence of giant impact formation of the Moon and the evolution of the lunar magma ocean (LMO), however, the details remain debated (Day et al., 2020; Kato et al., 2015; Paniello et al., 2012; Wang and Jacobsen, 2016). Recent detection of el- evated concentrations of volatile elements and water in various types of lunar materials have the potential to change the paradigm of a strongly volatile depleted Moon (Chen et al., 2015; Hauri et al., 2015; Ni et al., 2019; Saal and Hauri, 2021). New estimates of the lunar mantle composition propose depletion factors of only 2 to 5 for volatile elements when compared to the bulk silicate Earth (BSE). However, in order to balance the proposed models of a more volatile-rich lunar interior with the volatile depleted nature of most analyzed lunar samples, strong magmatic degassing is required (e.g., Chen et al., 2015; Hauri et al., 2015; Ni et al., 2019). Following this idea, the magnitude of stable isotope fractionation of different volatile elements in lunar mantle melts was interpreted by some authors to reflect variable degrees of magmatic degassing of lunar magmas (Saal and Hauri, 2021; Zhang, 2021).

Siderophile volatile elements (SVE) are of special interest, because in addition to their volatile nature they show variable affinities for metal and sulfide (Norris and Wood, 2017; Wood et al., 2014). Because core formation may have lowered their concentra-

tions in the lunar silicate portion substantially (e.g., Righter, 2019; Steenstra et al., 2017), they can potentially provide constraints on late accreted material and its volatile content (e.g., Wang and Becker, 2013, 2017). However, SVE may have been fractionated during silicate differentiation processes and variable extents of volatile loss. Although magmatic degassing is evident from abundant vesicles in lunar mare basalts and volatile-rich coatings on pyroclastic glass beads and highland rocks, the nature of the gas phase and its ability to effectively transport volatile metals is still debated (e.g., Day et al., 2019; Goldberg et al., 1976; Krähenbühl et al., 1973; McCubbin et al., 2015; Renggli and Klemme, 2021). Advances in this field require a better understanding of SVE inventories of pristine lunar rocks. The latter are presumably endogenous, magmatic rocks that underwent limited or no secondary melting by impacts and very little contamination with impactor material as gauged by very low mass fractions of highly siderophile elements (HSE) (Warren, 1993). Unfortunately, a thorough assessment of existing SVE mass fraction data of these samples is often hampered by analytical issues, where variable mass fractions have been obtained by different analytical methods and key elements like S and Cu were either not determined at all or not from the same sample aliquot.

In this study, we present a different perspective on the lunar volatile inventory based on new siderophile volatile element data (Cu, Se, Ag, S, Te, Cd, In, Tl) determined by isotope dilution inductively coupled plasma mass spectrometry (ICP-MS) on samples of the main pristine magmatic lithologies of the lunar crust. The data show a coherent picture of SVE behavior in different lunar magmatic rock series on which subsequent chemical and isotopic studies can build upon. With the new compositional data, we close a gap in knowledge and make it easier to evaluate older data like those obtained by radiochemical neutron activation analysis (RNAA). We show that this approach improves our understanding of SVE inventories of different lunar mantle reservoirs as well as the influence of magmatic differentiation and degassing on lunar magmatic rocks.

2. Materials and methods

In this study we analyzed mare basalts and pristine highland rocks. In general, the textural, chemical, and isotopic compositions of different samples allow the identification of different cogenetic magmatic suites (see also Supplementary Material 1). Apollo 12 mare basalts belong to the low-Ti olivine basalt suite, which formed 3.16 ±0.01 Ga ago (Snape et al., 2019). The strong positive correlation of grain size with normative olivine content in Apollo 12 olivine basalts was interpreted as the result of fractional crystallization and accumulation of olivine in the basal portion of a cooling basalt flow (Walker et al., 1976). Apollo 15 mare basalts belong to the low-Ti olivine-normative basalt suite, which crystallized 3.29 ±0.01 Ga ago (Snape et al., 2019). Their chemical variability is attributed to fractional crystallization of mainly olivine within a shallow magma chamber and extrusion as a sequence of thin lava flows (Ryder and Schuraytz, 2001). Consequently, samples of both mare basalt suites evolve along olivine fractionation lines (Fig. 1). Basalts with moderate MgO contents (~11 wt.%) like 12009, 15016, and 15555 are considered as unfractionated basalt liquidus compositions (Rhodes et al., 1977; Ryder and Schuraytz, 2001; Walker et al., 1976). In contrast, picritic basalts with higher MgO contents like 12020 (13.9 wt.%) and 12040 (16.7 wt.%) were interpreted as cumulate-melt mixtures (Rhodes et al., 1977; Walker et al., 1976). Some mare basalts like 15016 and 15556 comprise up to 50 vol.% vesicles, interpreted as remnants of a magmatic gas phase (e.g., Goldberg et al., 1976). Apollo 17 mare basalts belong to distinct high-Ti basalt flows that formed in a short time interval from 3.75 to 3.76 Ga ago (Snape et al., 2019).

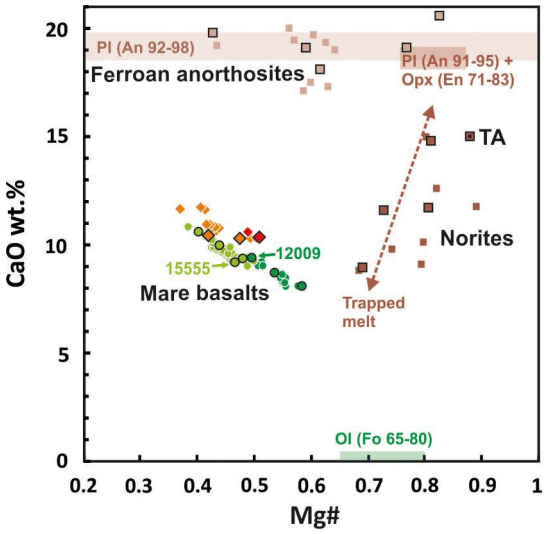

Fig. 1. Mg# (molar Mg/(Mg+Fe^{2+}) ratio) *vs.* mass fractions of CaO in lunar mare basalts and pristine highland rocks. Literature XRF data for representative mare basalt suites (green: Apollo 12 olivine basalts, light green: Apollo 15 olivine-normative basalts, orange: Apollo 17 type B basalts, red: Apollo 17 type C basalts) and INAA data for highland rocks (light brown: ferroan anorthosites, dark brown: magnesian norites) compiled from the lunar sample compendium (Meyer, 2010). Samples of this study are indicated by black frames. Samples of the magnesian suite are noritic, except of one troctolitic anorthosite (TA, see text for details). The ranges of Mg# in olivine of low-Ti mare basalts, CaO in plagioclase of ferroan anorthosites, and Mg# of low-Ca pyroxene combined with CaO in plagioclase of magnesian norites are shown for comparison. (For interpretation of the colors in the figure(s), the reader is referred to the web version of this article.)

Trace element modeling and experimental petrology suggest that they formed from low degree partial melting of ilmenite-bearing source compositions and evolved along similar fractional crystallization trends (e.g., Neal et al., 1990).

In addition to mare basalts, which are often considered in SVE studies, we include plutonic rocks of the magnesian suite and flotation cumulate rocks of the ferroan anorthosite suite because of their different origins and different cooling histories. Based on chemical data and petrographic observations Warren (1993) assessed high pristinity confidence levels of 8-9 for all highland samples of this study except for 61015 and 76255, which have been assigned a confidence level of 6. Anorthosite samples of this study (15415, 60025, 61015, 62255, 65315) have calcic plagioclase (An 92-98) abundances >95 vol.% (Fig. 1), minor mafic silicates (Mg# <0.74) and REE concentrations <3×CI chondrite, i.e., they are all ferroan anorthosites *sensu stricto*. The often cataclastic anorthosites were interpreted as monomict to polymict breccias of coarse-grained precursor anorthosites, but without significant admixture of other lithologies (e.g., Floss et al., 1998). The magnesian suite samples of this study are troctolitic anorthosite (76335), anorthositic norite (15455) norites (77215, 78235), and a gabbronorite (76255) which display variable modal abundances of cumulate plagioclase (48-88 vol.%; An 91-95), olivine and/or low-Ca pyroxene (30-51 vol.%; En 71-83; Fig. 1). Minor high-Ca pyroxene and other interstitial phases are considered to have crys- tallized from trapped intercumulus melt (e.g., Shearer et al., 2015). Magnesian suite rocks have been exhumed from depth by large impacts and most samples are clasts in polymict impact melt brec- cias (Shearer et al., 2015). Petrographic observations indicate only moderate shock pressures for the studied magnesian suite samples, except for norite 78235 where much of the plagioclase is converted to diaplectic glass.

Sample preparation, digestion, chemical separation, and analyses were conducted in the Geochemistry laboratories at Freie Universität Berlin, Germany, following procedures established pre-

Table 1
Mass fractions of siderophile volatile and refractory lithophile trace elements in lunar pristine highland rocks and mare basalt samples.

		Weight [g]	Sm [µg/g]	Ba [µg/g]	Cu [µg/g]	Se [ng/g]	Ag [ng/g]	S [µg/g]	Te [ng/g]	Cd [ng/g]	In [ng/g]	Tl [ng/g]
Low-Ti mare basalts												
12009,173	OB	0.20691	3.77(2)	60.9(2)	5.42(6)	145(1)	0.88(12)	744(5)	2.45(3)	0.657(10)	0.816(9)	0.511(5)
12020,537#1	OB	0.26208	4.54(2)	63.8(1)	5.23(5)	146(1)	0.847(92)	776(4)	2.57(2)	0.487(9)	1.46(1)	0.464(4)
12020,537#2	OB	0.26002	3.46(2)	50.5(1)	4.51(4)	115(1)	0.660(92)	612(4)	1.71(2)	0.480(8)	1.30(1)	0.318(4)
12020,537#3	OB	0.16956	3.12(1)	50.7(2)	4.59(7)	111(1)	0.77(14)	583(6)	1.74(3)	0.526(12)	2.01(1)	0.210(6)
12020,537 av.	OB		3.79(2)	55.6(1)	4.80(5)	126(1)	0.76(10)	667(5)	2.04(2)	0.494(9)	1.54(1)	0.347(4)
12040,237	OB	0.25713	2.72(1)	38.2(1)	4.07(5)	105(1)	0.605(93)	552(4)	0.924(19)	0.396(8)	0.238(5)	0.143(4)
15016,247	ONB	0.25527	2.51(1)	42.1(1)	7.99(5)	116(1)	1.72(3)	682(2)	1.81(3)	0.379(17)	0.259(34)	0.232(8)
15555,1103	ONB	0.25043	2.66(1)	41.0(1)	6.41(4)	108(1)	0.660(31)	629(2)	1.44(3)	0.259(17)	0.322(35)	0.226(8)
15556,289	ONB	0.24510	3.57(1)	51.7(1)	8.55(5)	148(1)	0.789(31)	852(2)	1.90(3)	2.51(2)	0.543(36)	0.257(8)
15557,157	ONB	0.24937	3.50(1)	50.5(1)	7.96(4)	140(1)	0.841(31)	807(2)	1.94(3)	0.351(17)	0.519(35)	0.285(8)
High-Ti mare basalts												
70215,58	Type B	0.24917	6.55(4)	61.3(2)	5.21(5)	189(1)	1.01(10)	1800(7)	1.83(2)	1.31(1)	0.687(5)	0.256(4)
74255,227	Type C	0.25173	5.57(3)	55.8(2)	3.18(5)	151(1)	0.526(95)	1200(5)	1.45(2)	1.08(1)	0.494(5)	0.120(4)
75075,41	Type B	0.24344	4.70(2)	49.0(1)	3.92(5)	157(1)	0.662(99)	1478(6)	1.33(2)	0.994(10)	0.149(5)	0.255(4)
Ferroan anorthosites												
60025,922 #1	cat.	0.51890	0.207(1)	11.6(1)	0.634(7)	4.19(16)	b.d.l.	43.3(6)	14.4(1)	31.9(3)	219(1)	48.7(1)
60025,922 #2	cat.	0.47070	0.245(2)	10.6(1)	0.879(6)	5.40(18)	b.d.l.	54.4(7)	18.8(1)	28.4(2)	186(1)	45.7(3)
60025,922 av.	cat.		0.225(2)	11.1(1)	0.751(6)	4.77(17)	b.d.l.	48.6(7)	16.5(1)	30.2(3)	203(1)	47.3(2)
65315,170 #1	cat	0.43800	0.0963(6)	5.36(3)	0.274(6)	7.30(13)	1.78(11)	32.4(7)	0.410(23)	330(2)	40.5(3)	53.8(4)
65315,170 #2	cat	0.51891	0.0913(5)	6.06(2)	0.236(5)	6.88(16)	1.70(9)	30.2(6)	0.545(20)	398(2)	49.8(2)	63.2(4)
65315,170 av.	cat.		0.0936(6)	5.74(3)	0.254(6)	7.07(15)	1.73(10)	31.2(7)	0.483(21)	367(2)	45.5(2)	58.9(4)
15415,273		0.50570	0.0750(6)	5.97(5)	b.d.l.	b.d.l.	0.542(27)	b.d.l.	0.0129(33)	3.10(3)	b.d.l.	0.0655(10)
61015,209		0.32288	0.217(1)	11.1(9)	0.212(46)	15.2(2)	0.425(42)	74.9(1.0)	6.30(4)	1.70(2)	1.71(12)	20.3(1)
62255,314		0.50150	0.173(1)	11.3(1)	0.238(30)	0.41(11)	0.203(27)	4.45(59)	1.23(1)	14.4(1)	2.67(8)	40.5(2)
Magnesian suite												
15455,395	AN	0.52214	0.664(5)	32.1(3)	0.320(28)	9.06(11)	1.09(3)	62.5(6)	0.735(9)	2.08(2)	b.d.l.	0.339(2)
76255,132	cat. GN	0.48662	5.29(4)	141(1)	1.41(3)	52.4(1)	704(28)	419(1)	784(7)	1.04(2)	0.266(78)	0.621(3)
76335,82	cat. TA	0.49783	0.832(9)	44.5(3)	0.102(30)	0.19(12)	0.191(27)	9.00(60)	0.0661(37)	0.836(18)	b.d.l.	0.041(3)
77215,298	cat. N	0.50126	3.75(2)	371(1)	2.76(3)	73.8(2)	1.18(3)	504(1)	0.664(11)	3.08(2)	0.241(76)	0.315(2)
78235,170	sh. N	0.49740	1.24(1)	40.1(4)	0.432(30)	18.9(1)	0.413(27)	71.3(6)	1.43(4)	1.22(2)	0.363(76)	0.0176(10)

Uncertainties on mass fractions, estimated based on the precision of measured isotope ratios and the uncertainty of blank averages, are given in parentheses (2σ) and refer to the last decimal places. Measured total analytical blank values and details of the calculation of procedural detection limits are given in the Supplementary Material 2. Abbreviations: AN – anorthositic norite, av. - average (weighted), b.d.l. – below detection limit, Cat. – cataclastic, GN – gabbronorite, N – norite, OB – olivine basalt suite, ONB – olivine-normative basalt suite, Sh. – shocked, TA – troctolitic anorthosite.

viously for terrestrial rocks, Martian meteorites, and chondrites (Wang and Becker, 2015, 2017; Wang et al., 2015). Samples and isotopic tracer solutions have been digested and equilibrated in HF-HNO_3 in Parr bombs, analyte elements were separated from the rock matrices by anion and cation exchange chromatography, and were measured by ICP-MS. We thoroughly monitored total analytical blanks throughout the study. All concentrations were corrected for average blank contributions, which accounts mostly for <10% of analyzed SVE. Uncertainties have been calculated based on the precision of measured isotope ratios and the uncertainties of average blank contributions and are below 5% for the most elements. Calculated uncertainties are higher in samples with very low concentrations (Mare basalts: uncertainties on Ag of up to 20%. Highland rocks: uncertainties on Ag, S, and Se of up to 60%). Details of the procedures are outlined in the Supplementary Material 2.

3. Results

Mass fractions of SVE (Cu, Se, Ag, S, Te, Cd, In, Tl) and two refractory lithophile trace elements (Sm, Ba) were determined from the same sample aliquot of 10 mare basalts, 5 magnesian suite rocks, and 5 ferroan anorthosites (Table 1). Samarium, Ba, Cu, and S are in the µg/g range whereas all other elements are in the lower ng/g range. Similar mass fractions were determined for SVE by RNAA (e.g., Krähenbühl et al., 1973; Wolf et al., 1979) and for S by XRF (e.g., Rhodes et al., 1977). In contrast, 3 to 10 times higher mass fractions were determined for Cu by external standardization ICP-MS (see Supplementary Material 3). In this study, we provide the first comprehensive data set for SVE in lunar samples, including Cu and S, determined by the same method from the same digestion aliquot.

When normalized to average CI chondrite values, mass fractions of analyzed SVE display distinct fractionation patterns between the main magmatic lithologies. Low-Ti mare basalts display very similarly fractionated SVE patterns showing increasing depletions in the order of Cu<S<Se ≤ In ≤ Ag ≤ Tl ≤ Cd ≤ Te (Fig. 2a). High-Ti mare basalts display mass fractions and normalized patterns broadly similar to low-Ti mare basalts, but with higher abundances of S, Se, and Cd (Fig. 2b). Gabbronorite, anorthositic norite, and norite samples of the magnesian suite (hereinafter collectively termed magnesian norites) display lower mass fractions for most SVE than mare basalts, but broadly similar fractionation patterns from Cu to Te (Fig. 2c). The troctolitic anorthosite 76335 of the magnesian suite displays the lowest mass fractions of Cu, Se, Ag, S, and Te, but is similar in Cd and Tl. In contrast, samples of the ferroan anorthosite suite display the strongest fractionations between different SVE (Fig. 2d). Whereas Cu, Se, Ag, and S are in the range of magnesian suite rocks, strong enrichments of Te, Cd, In, and Tl occur in most samples.

When compared to incompatible lithophile trace elements like Sm (Fig. 3) and bulk rock Mg# (Fig. 4) the different basalt suites display distinct correlations for some SVE. Positive correlations with Sm and negative correlations with Mg# are observed for Cu, S, Se, and Ag (Fig. 3b-d and 4b-d). Although discernible in some cases, correlations are less well defined for Te, Cd, In, and Tl (Fig. 3e, f and 4e, f). In magnesian suite samples different SVE display only weak or no correlation with Sm, however Cu, S, and Se yield well-defined negative correlations with Mg# (Fig. 4b-c). Ferroan anorthosites display Cu/Sm, S/Sm, and Se/Sm ratios in the

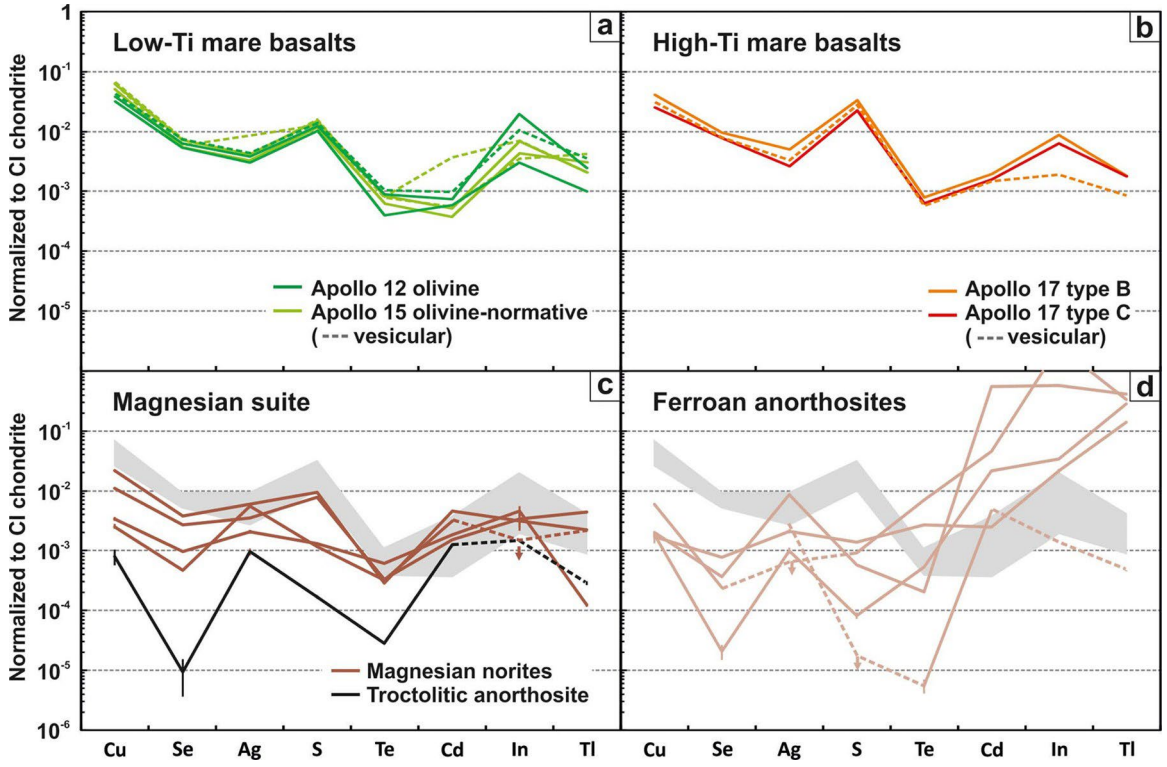

Fig. 2. Mass fractions of siderophile volatile elements in mare basalts (a and b) and magmatic highland rocks (c and d) normalized to the CI chondrite Ivuna (Wang et al., 2015). For samples where more than one aliquot was measured, weighted averages are shown. For comparative purposes, elements are arranged according to decreasing 50% condensation temperatures from a gas of solar nebular composition (Wood et al., 2019). In panel (c) and (d) the mare basalt range (gray field; n=10) is displayed for comparison. When neighboring elements are not determined in highland samples (panel d and c), dotted lines link to the respective detection limit.

range of studied mare basalts, but the values are higher than in magnesian suite rocks (Fig. 3b-c).

Ratios of SVE with different affinities to metal, sulfide and gas phase reveal systematic differences between the main magmatic lithologies as well as between different mare basalt suites. Apollo 12 olivine basalts, Apollo 15 olivine-normative basalts, and Apollo 17 type B basalts display very tight clusters in Cu/Se, S/Se, Cu/S, Cu/Ag, and Se/Ag ratios (Fig. 5). In contrast Ag/Cd, Se/Tl and Ag/Tl ratios are more variable (up to factor of 15). The Apollo 17 type C basalt sample is often similar to the type B basalt samples. Magnesian suite rocks display variability in their Cu/S, Cu/Se, and S/Se ratios and are in the range of mare basalts. On the other hand, for ratios like Cu/Cd, Ag/Cd, Se/Tl, and Ag/Tl most magnesian norites fall close to the composition of impact melt breccia boulders in which they were enclosed as clasts (Fig. 5a-c). Notably the shocked norite sample 78235 displays a factor of 5 higher Se/Tl and Ag/Tl ratios than all other magnesian norites and the impact melt breccia boulders (Fig. 5c). Ferroan anorthosites are characterized by variable Cu/Se, Cu/S, and S/Se ratios, which mostly exceed the range of the mare basalts and the magnesian suite rocks (Fig. 5a). Because of the strong enrichment of Cd and Tl, ferroan anorthosite samples cluster at very low Cu/Cd, Ag/Cd, Se/Tl, and Ag/Tl ratios (Fig. 5b and c).

4. Discussion

4.1. Siderophile volatile element inventory of lunar magmatic rocks

4.1.1. Silicate differentiation

Crystallization of the LMO produced distinct chemical reservoirs like dense mafic cumulates, buoyant plagioclase cumulates, very dense ilmenite bearing cumulates, and residual KREEP, rich in lithophile incompatible trace elements like potassium, rare earth elements, and phosphorus. (e.g., Elkins-Tanton et al., 2011). Overturn of the LMO cumulate pile before the end of complete solidification presumably led to decompression melting of early magnesium-rich LMO cumulates and hybridization with KREEP at the base of the crust (Elkins-Tanton et al., 2011). These parental melts of the magnesian suite intruded the early lunar crust and underwent slow cooling and fractional crystallization under lithostatic pressures (Shearer et al., 2015). Mare basalts formed by low degrees of partial melting of cumulate sources significantly after LMO solidification. Differences in the relative amounts of primary LMO cumulate phases and trapped LMO liquid in the mantle sources of mare basalts exert the dominant control on their chemical and isotopic compositions (Hallis et al., 2014; Shearer et al., 2006; Snape et al., 2019). Pyroclastic glasses most likely represent a minor, but nevertheless relevant fraction of lunar magmatism, because they are more Mg-rich and formed at greater depths than the mare basalts (Shearer et al., 2006). Effusion of mare basalt flows and pyroclastic eruptions under very low-pressure conditions of the lunar surface are expected to facilitate degassing when compared to plutonic rocks of the magnesian suite.

Since mantle material is currently not available for study, the composition of the lunar interior must be constrained from mantle derived mafic rocks. Mass fractions of refractory lithophile elements (RLE) as well as Mg# (magnesium number, molar $Mg/(Mg+Fe^{2+})$ ratio) are used to trace back partial melting of the LMO cumulates and differentiation of mantle melts. In Fig. 3, Sm is used because it is incompatible in most silicate phases and refractory (i.e., abundances were not affected by volatilization, Wood et al., 2019). In Fig. 4, the new trace element data are compared to Mg# data compiled from the literature. In mare basalts lithophile Ba is well correlated with Sm (Fig. 3a), consistent with fractional crystallization of mainly olivine (Fig. 4a). Ratios of Ba/Sm distinguish low-Ti basalts (14-17) from high-Ti basalts (~10), which was interpreted earlier to result from differences in mantle source compositions (Rhodes et al., 1977). Magnesian suite rocks are charac-

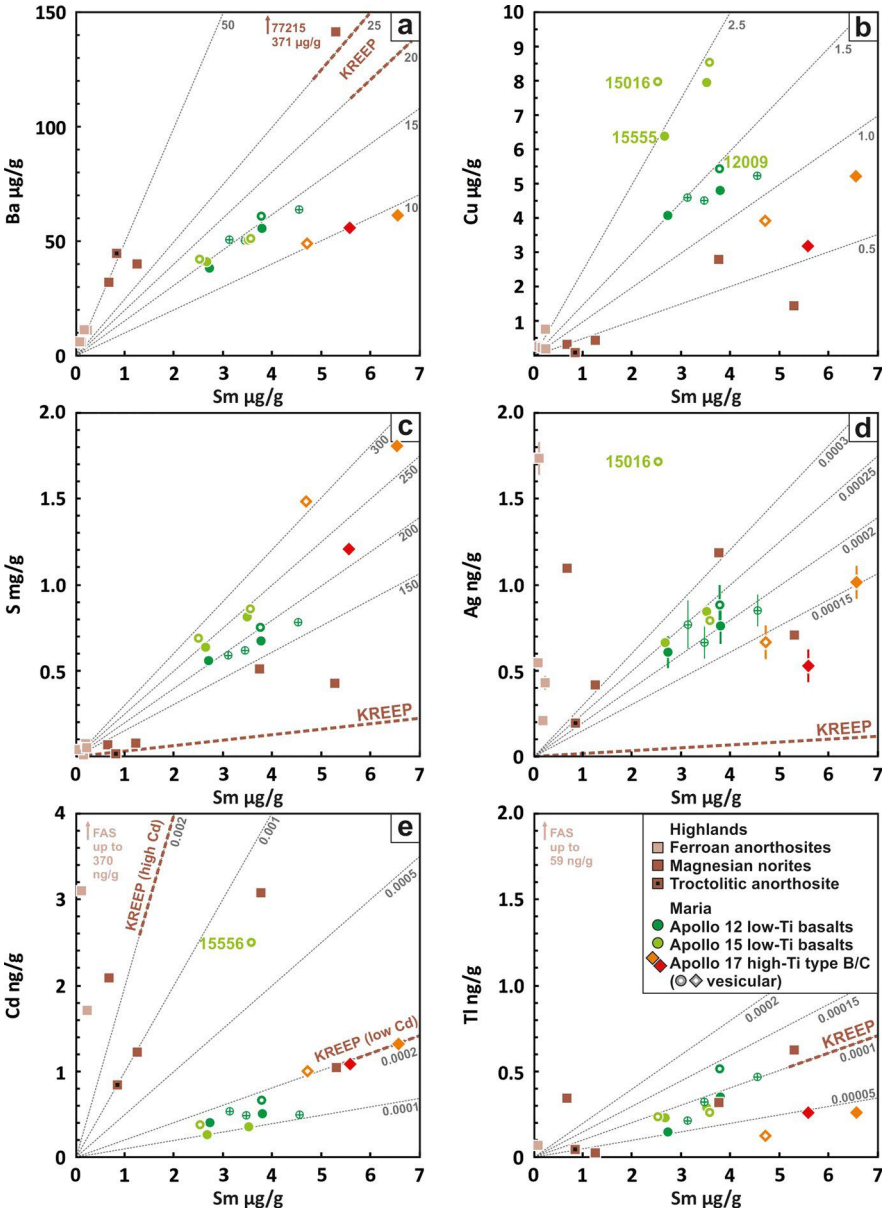

Fig. 3. Isotope dilution ICP-MS trace element data obtained during this study (2σ uncertainties are shown when larger than symbol size). For Apollo 12 low-Ti mare basalt 12020, data for all three aliquots are shown together with the weighted average. Element ratios in average KREEP basalts are shown for comparison (for display of Se, Te, and In data and KREEP basalt data source see Supplementary Material 3; note: no reliable data for Cu in KREEP basalts are available).

terized by Ba/Sm ratios >25, consistent with their formation from hybrid mantle melts with variable KREEP components (Shearer et al., 2015). Ferroan anorthosites display the lowest mass fractions of most trace elements, but the highest Ba/Sm ratios (50-80), consistent with available plagioclase trace element data and formation by accumulation of plagioclase (Floss et al., 1998).

In contrast to RLE, which in magmatic rocks are controlled by fractional crystallization of silicate, oxide, and phosphate phases, SVE are hosted mainly in accessory sulfides and metal and their mass fractions may have been lowered by unknown degrees of magmatic degassing. For most SVE we find positive correlations with Sm (Fig. 3b-f) and negative correlations with Mg# (Fig. 4b-f) in the different mare basalt suites of this study. Both systematics indicate incompatible behavior of the SVE during fractional crystallization similar to lithophile incompatible trace elements (Fig. 3a and 4a). This is most prominent for the more abundant SVE like Cu, S, and Se, but also discernible for elements in the lower ng/g range like Ag. Therefore, we argue that in different mare basalt suites SVE are mainly controlled by fractional crystallization. In general, correlations of SVE with Sm are less well defined than with Mg#. This is most likely because of the variable dissemination of accessory sulfides and phosphates in the analyzed rocks. Comparison of basalts with different MgO contents clearly reveals that in Apollo 12 olivine basalts and the Apollo 15 olivine-normative basalts the SVE follow olivine control lines (Fig. 4). Furthermore, olivine-hosted melt inclusion data for sulfur in both mare basalt suites lie onto or close to the olivine control lines defined by the bulk rock data of this study (Fig. 4c). In contrast, bulk rock and melt inclusion data for SVE in the lower µg/g range, which have been determined with other methods display unsystematic distribution and most likely reflect analytical problems (e.g., Cu in Fig. 4b). In high-Ti basalts, the concomitant fractional crystallization of olivine and FeTi-oxides (Neal et al., 1990) produces a steeper slope in SVE-Mg# diagrams than for low-Ti basalts (Fig. 4), the exception being Cu, because it is only mildly incompatible in FeTi-oxides (Dygert et al., 2013).

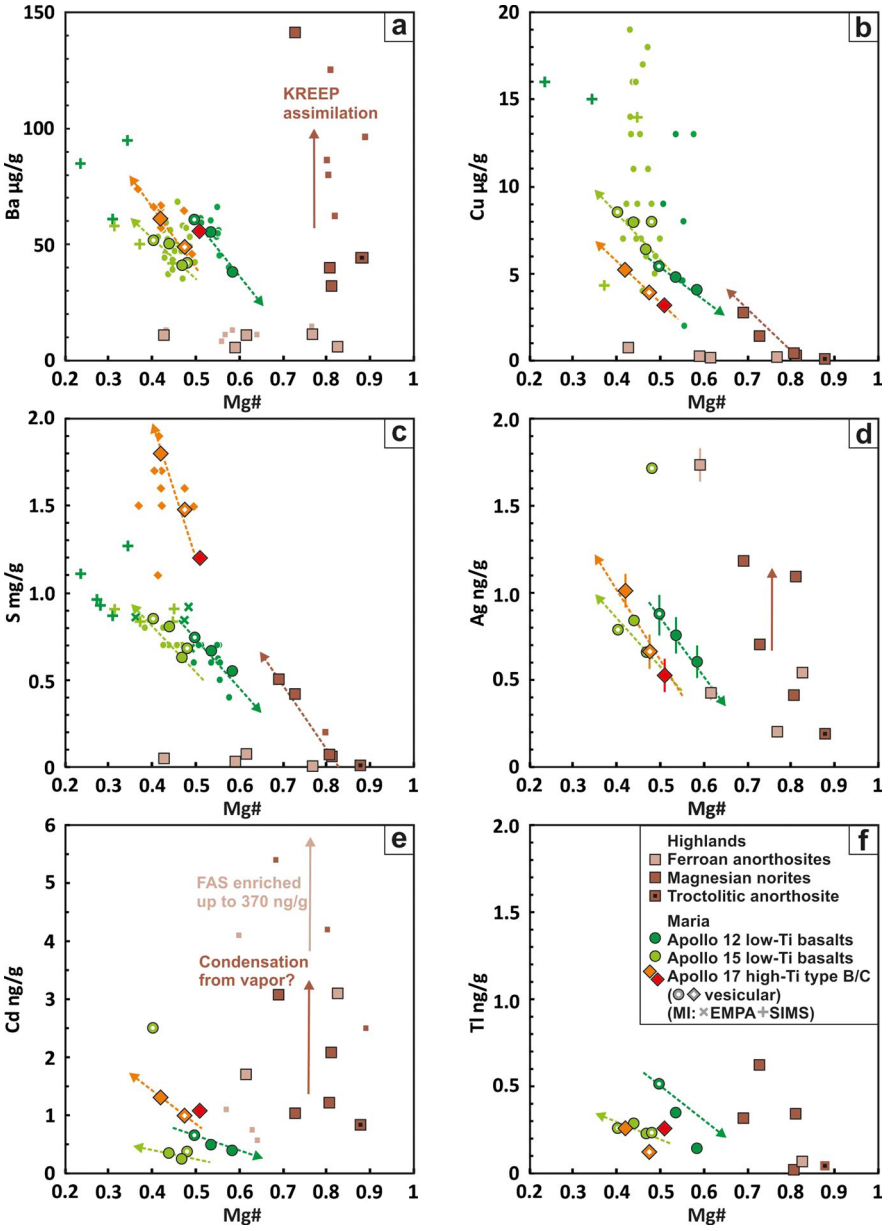

Fig. 4. Mg# (molar Mg/(Mg+ Fe^{2+}) ratio) *vs.* mass fractions of refractory lithophile elements and siderophile volatile elements in lunar mare basalts and pristine highland rocks (for display of Se, Te, In, and Sm data see Supplementary Material 3). Representative XRF and INAA data from the literature are displayed by smaller symbols (compiled from the same data set as in Fig. 1). In panel (a-c) olivine-hosted melt inclusion (MI) data (Bombardieri et al., 2005; Ni et al., 2019) for samples that were analyzed also in the present study are shown for comparison. Note: melt inclusion Cu data are often higher than 10 µg/g and might reflect matrix effects in SIMS measurements (Ni et al., 2019). Uncertainties for SIMS and EMPA data are not reported, but are at least 10% or higher. Fractional crystallization trends (dotted lines) are fitted through the proposed parent melt compositions and olivine (12009/Fo75 and 15555/Fo70) in low-Ti basalts, two type B basalts and olivine (Fo65) in high-Ti basalts and the data array and low-Ca pyroxene (En83) for magnesian norites. Hybridization of highland rocks due to assimilation of KREEP and/or interaction with a vapor phase is shown schematically (solid lines).

The major element composition of the studied magnesian norites clearly indicates variable fractions of cumulate phases and trapped melt in these rocks (Fig. 1). Mass fractions of SVE broadly scale with the amount of trapped melt and fractionation patterns reveal a striking similarity between magnesian norites (and by implication their parent magmas) and mare basalts (Fig. 2c). Furthermore, four magnesian norites display a negative correlation with Mg# parallel to low-Ti mare basalts for Cu, S, and Se, but not for Ba and Sm (Fig. 4 and Fig. S6). Although the different magnesian norites are not cogenetic, this observation can be explained by fractional crystallization of low-Ca pyroxene and plagioclase from mantle melts with similar major element composition and very similar abundances of Cu, S, and Se. In contrast, RLE in magnesian norites are not easily explained by fractional crystallization and most likely reflect variable hybridization and entrapment of KREEP as was suggested earlier (e.g., Shearer et al., 2015). The contrasting behavior between chalcophile and lithophile trace elements in KREEP-bearing magnesian norites, suggests that their SVE inventories are not related to assimilation of KREEP. This is further supported by higher SVE/Sm ratios in magnesian norites except for Cd/Sm and Tl/Sm which overlap with average KREEP basalts (Fig. 3). However, KREEP basalt data are limited and mass fractions vary by up to a factor of 10 for the more volatile SVE. Although considered as pristine, most magnesian suite samples were in close contact with impact melt (see Supplementary Material 1) and minor contamination with impactor material is clearly visible in their HSE inventory (Day et al., 2010). However, minor impactor contributions, most likely had only little effect on the more abun-

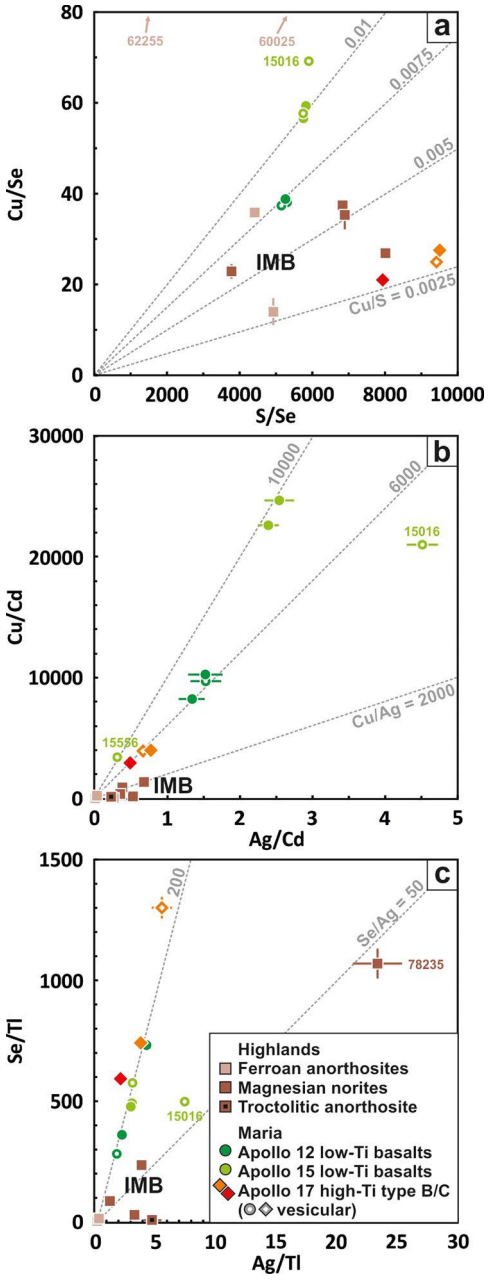

Fig. 5. Ratios of SVE with different affinities to metal, sulfide, and gas phase. The composition of Apollo 17 impact melt breccia boulders (IMB) are displayed schematically (see Supplementary Material 3 for references).

dant SVE like S and Cu, whereas mass fractions and element ratios of less abundant and more volatile SVE overlap with the composition of impact melt breccia boulders (Fig. 5b and c; see discussion below).

The composition of ferroan anorthosites is dominated by cumulate plagioclase which makes up more than 95 vol.% of the rocks. Therefore, concentrations of incompatible elements are generally low. Element ratios like Cu/Sm, S/Sm, and Se/Sm fall in the range of mare basalts (Fig. 3b and c) and suggest a similar relation to silicate melt differentiation. However, if this is due to trapping of small amounts of LMO liquid (Floss et al., 1998), metasomatism by hybrid melts (Elkins-Tanton et al., 2011) or due to admixture of mafic material during later brecciation remains ambiguous. In contrast, the variable enrichments of other SVE like Ag, Te, Cd, In, Tl and their overall high SVE/Sm ratios (Fig. 3d-f) cannot be reconciled by silicate melt differentiation and require a different explanation (see discussion below).

4.1.2. *Sulfide-metal-silicate partitioning of the magmas*

In mare basalts, mass fractions of Cu, S, Se, and Ag are well correlated to indicators of fractional crystallization (Fig. 3 and 4). Similar relationships can be observed in sulfide-undersaturated terrestrial komatiites (e.g., Puchtel et al., 2016) and in some Martian shergottites (Wang and Becker, 2017). The correlation of these siderophile and strongly chalcophile elements with indicators of magmatic fractionation rules out that late-magmatic sulfide or metal segregation significantly affected such magmas (as was also argued by Day, 2018). This notion is also supported by similar Cu/S ratios of Apollo 12 olivine basalts (0.0072-0.0074, Fig. 5a) and sulfide globules in experimentally heated olivine-hosted melt inclusions in one of these samples (0.0064-0.0089, Bombardieri et al., 2005). These results suggest that there was no significant post-entrapment modification of Cu in the host magma by sulfide segregation. Recent *in-situ* analyses of magmatic phases in Apollo 15 olivine-normative basalt sample 15555 reveal strong differences in Cu/Se ratios between metal and troilite grains (Day and Paquet, 2021). Accumulation of tiny metal grains trapped in early formed olivine could potentially explain the high Cu/SVE ratios observed in the Apollo 15 olivine-normative basalt suite (Fig. 5a, b). However, petrographic observations suggest that metal and troilite formed throughout the crystallization sequence and that the fraction of metal in early formed olivine is small (Day and Paquet, 2021). This observation is consistent with results of the present study and suggests that elevated Cu/SVE ratios are a feature of the parent melt. A comparison of the different mare basalt suites yields systematically decreasing Cu/Se, Cu/S, Cu/Cd, and Ag/Cd ratios from Apollo 15 olivine-normative basalts to Apollo 12 olivine basalts to Apollo 17 type B basalts (Fig. 5). The latter fractionations between elements with different affinities to sulfide, metal, and gas phase indicate that silicate-sulfide-metal partitioning processes and/or degassing could have affected some of these magmas at an earlier stage of their evolution, or chemical differences between their mantle sources exist (this topic will be discussed in section 4.3 in more detail). A prerequisite for further evaluation of these scenarios is a better understanding of the influence of magmatic degassing on SVE inventories.

4.2. *Assessing the role of magmatic degassing*

4.2.1. *Mare basalts*

The well-preserved correlation of Cu, S, Se, and Ag mass fractions with indicators of silicate melt differentiation strongly suggests that fractional crystallization exerts the dominant control on SVE in mare basalts and that late-magmatic metal and/or sulfide saturation did most likely not occur (see discussion above). However, this also shows that these specific elements were modified only little or not by late-magmatic degassing. For example, vesicular mare basalts, which are believed to be more degassed than non-vesicular basalts, mainly follow the fractional crystallization trends and are not characterized by SVE depletions (Fig. 4). In addition, the new data reveal systematic differences in SVE ratios between different mare basalt suites, which are not resolvable in older data (Fig. 5a and b). Apollo 12 olivine basalts, Apollo 15 olivine-normative basalts and Apollo 17 type B basalts display tight clusters of their Cu/Se, Cu/S, S/Se, Cu/Cd, Cu/Ag, and Ag/Cd ratios (Fig. 5a and b). Such systematic differences between basalt suites are inconsistent with late magmatic degassing, in particular because elements like Ag and Cd display very similar degassing behavior in reduced mafic melts (Norris and Wood, 2017). Nevertheless, some of the less abundant and more volatile SVE display variable deviations from olivine control lines. Silver and Cd, which

generally follow fractional crystallization trends, are sometimes enriched in vesicular Apollo 15 mare basalt samples (Fig. 4d and e). Because other elements are not affected and characteristic element ratios of their basalt suite are preserved (Cu/Cd in 15016, Cu/Ag in 15556, Fig. 5b), we argue that these singular enrichments reflect traces of vapor-deposited Cd and Ag phases within the vesicle linings (Goldberg et al., 1976). In contrast, Te, In, and Tl are not always well correlated with Sm (Fig. 3f) or Mg# (Fig. 4f) and element ratios like Cu/Tl, Se/Tl, Ag/Tl vary significantly (Fig. 5c). Since this observation is similar in all three basalt suites we argue that fractional crystallization trends for Te, In, and Tl were partially disturbed by late-magmatic degassing or post-crystallization redistribution.

Correlations with indicators of fractional crystallization clearly excludes late-magmatic degassing for some SVE (S, Cu, Se, Ag, and partially Cd) in mare basalts, but cannot rule out that volatilization-related fractionation of SVE occurred earlier. Our new data show that considerable variability exists among SVE/RLE ratios (Fig. 3) and SVE ratios (Fig. 5) between different lunar mantle melt groups. These differences strongly argue for inherited compositional heterogeneities between different parent melt compositions. According to experimental data on reduced mafic melts, Cu is less volatile than most other SVE analyzed in this study (Norris and Wood, 2017). Therefore, the variability in Cu/SVE ratios between different mare basalt suites might have been caused by magmatic degassing prior to the onset of fractional crystallization. Because they are protected from volatile loss, olivine-hosted melt inclusions (i.e., former melt trapped within crystals) turned out to be a promising tool to understand pre-degassing volatile element abundances of lunar mantle melts. Sulfur concentrations of experimentally heated melt inclusions are commonly interpreted as primary magmatic compositions and the discrepancy to lower S contents of whole rocks was taken as evidence for late-magmatic degassing (Bombardieri et al., 2005; Ni et al., 2019). However, our new data show that whole rocks and melt inclusions of two different low-Ti mare basalt suites fall on olivine control lines without indications of significant S-loss due to degassing (Fig. 4c). Furthermore, we note that RLE like Ba also show higher mass fractions in melt inclusions than in their whole rocks (Fig. 4a). This, together with the low Mg# of most melt inclusions, suggests that their composition is possibly more strongly affected by post-entrapment crystallization than previously thought. In contrast to mare basalts, pyroclastic glasses provide unequivocal evidence for substantial loss of volatile elements like H, C, Cl, F, and S (McCubbin et al., 2015). The late-stage magmatic degassing of glass beads is facilitated by the small bead size and fast diffusion of the species (Saal and Hauri, 2021). Large sulfur isotope fractionations in these glass beads were interpreted as a result of open-system degassing during transport and eruption (Saal and Hauri, 2021). In contrast, only very limited stable S isotope fractionation was reported for mare basalts (Wing and Farquhar, 2015). This, together with the tight range in stable Zn isotope values, for which more data are available (e.g., Kato et al., 2015; Paniello et al., 2012), supports our interpretation that during effusion of mare basalt flows, degassing of SVE was less effective.

4.2.2. Highland rocks

The formation of plutonic magnesian suite rocks under lithostatic pressure prevented extensive magmatic degassing. This assumption is supported by systematic correlation of Cu, S, and Se with indicators of fractional crystallization (see discussion above). Furthermore, we note that Cu/Se, Cu/S, and S/Se ratios of magnesian norites fall in the range of mare basalts (Fig. 5a), which supports our interpretation that magnesian norites and mare basalts formed from similar parent magmas. Conversely, these similarities between plutonic and volcanic rocks suggest that degassing and fractionation during ascent and effusion of mare basalts was most likely limited for these elements. In contrast, in most highland rocks the more volatile SVE like Ag, Te, Cd, In, and Tl do not correlate with indicators of fractional crystallization (Fig. 3 and 4) and mass fractions suggest enrichment, rather than volatile loss. Based on element ratios we deduce different sequences of relative enrichment for magnesian suite rocks ($In<Tl<Ag<Cd$) and ferroan anorthosites ($Ag\approx Te<Cd\leq In\leq Tl$). In magnesian suite rocks replacement of mafic silicates with sulfides has been reported (e.g., in gabbronorite 76255) and was interpreted as secondary alteration resulting from interaction with S-rich vapor at shallow depths (Shearer et al., 2015 and references therein). In magnesian suite clasts from Apollo 17 impact breccia boulders Cu/Cd, Ag/Cd, Se/Tl, and Ag/Tl ratios fall in the range of adjacent impact breccia samples, which indicate that the impact breccia matrix is a likely source of the vapor phase. Following this interpretation, the S-rich vapor phase degassed from cooling volatile-bearing impact melt and caused sulfide replacement reactions in undigested highland clasts. Although norite 78235 is generally similar in SVE abundances to other magnesian suite rocks, its Se/Tl and Ag/Tl ratios are much higher (Fig. 5c) and were most likely caused by substantial loss of Tl due to shock heating.

The observed pattern for most ferroan anorthosite samples is very similar to sample 66095 'rusty rock', one of the most volatile-rich lunar rocks (Krähenbühl et al., 1973). However, in contrast to the extreme enrichment of the light isotopes of Zn in 'rusty rock', the isotopic composition of Cu and Fe fall within the previously reported range for lunar mare basalts (Day et al., 2019). This, together with concentration data suggests that 'rusty rock' interacted with a gas phase highly enriched in more volatile elements like Zn, Cd, and Tl, but depleted in less volatile elements like Fe and Cu (Day et al., 2019; Krähenbühl et al., 1973). Experimental data reveal that the 'rusty rock' alteration assemblage formed at $\sim$600° C due to interaction with a Zn-C-O-S-Cl gas phase (Renggli and Klemme, 2021). Based on the similarity of SVE patterns we argue that brecciated ferroan anorthosites interacted to variable degree with a similar gas phase like 'rusty rock'. This interpretation is supported by the wide range of Zn isotope ratios and mass fractions reported for some of the studied samples (Day et al., 2019; Kato et al., 2015).

4.3. Siderophile volatile elements in the lunar mantle

4.3.1. The composition of the low-ti mare basalt source

In mare basalts of this study, the systematic variation of Cu, S, Se, Ag, and partially Cd indicate limited degassing of these elements during fractional crystallization at shallow depths (see discussion above). Therefore, we argue that variations in Cu/Se, Cu/S, S/Se, Cu/Ag, Cu/Cd ratios between different mare basalt suites reflect compositional differences of their parent melts. We used two different methods to assess the inventory of SVE in mantle sources. In the first approach we use mass fractions of Cu, Ag, Se, S, and Cd in low-Ti basalt samples 12009 and 15555, which have been considered as close to parental melt compositions of their mare basalt suites (Rhodes et al., 1977; Ryder and Schuraytz, 2001). If the basalt compositions represent unfractionated basalt liquidus compositions mass, fractions of SVE in the respective mantle sources can be calculated as a function of the degree of partial melting. For example, for 5 to 15% of partial melting we obtain 32 to 94 μg/g S in the low-Ti mare basalt mantle sources (Table 2), comparable to the range of 10 to 92 μg/g estimated by Ding et al. (2018). In the second approach we compare mass fractions of SVE in studied mare basalts with RLE of similar incompatibility during mantle melting. The general assumption is that such volatile/refractory element ratios will be insensitive to differences in the degree of mantle melting and fractional crystallization and can be

Table 2
Mantle source compositions for low-Ti mare basalts.

	Melt[1]	Source composition of the Apollo 12 olivine basalt suite[2]			
	(12009)	5%	10%	15%	Regression
Cu µg/g	5.4	0.48	0.74	1.0	0.66
Ag ng/g	0.88	0.046	0.090	0.13	0.10
Se ng/g	145	7.3	15	22	14
S µg/g	744	37	74	112	72
Cd ng/g	0.66	0.096	0.13	0.16	0.070
Cu/Ag	6158(816)	10500	8220	7460	6600
Cu/S	0.0073(1)	0.0130	0.0100	0.0089	0.0092

	Melt[1]	Source composition of the Apollo 15 olivine-normative basalt suite[2]			
	(15555)	5%	10%	15%	Regression
Cu µg/g	6.4	0.56	0.87	1.2	1.5
Ag ng/g	0.66	0.034	0.067	0.10	0.15
Se ng/g	108	5.4	11	16	18
S µg/g	629	32	63	94	103
Cd ng/g	0.26	0.038	0.049	0.061	0.065
Cu/Ag	9712(454)	16500	13000	11800	10000
Cu/S	0.0102(1)	0.0175	0.0138	0.0126	0.0146

[1] Mass fractions of Cu, Ag, Se, and S in hypothetical unfractionated parental melt based on samples 12009 and 15555 (this study). Uncertainties on element ratios (propagated from uncertainties on concentration data in Table 1), are given in parentheses and refer to the last decimal places.

[2] Mass fractions in the mantle source have been calculated for non-modal batch melting model (5-15% partial melting) and a regression approach (for details see Supplementary Material 3).

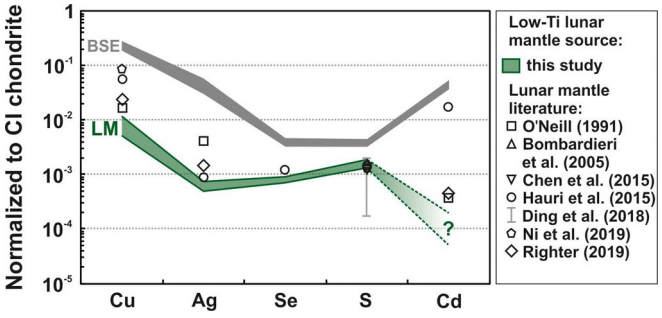

Fig. 6. Mass fractions of Cu, Ag, Se, S, and Cd in the mantle source of the Apollo 12 olivine basalt suite and the Apollo 15 olivine-normative basalt suite (Table 2, regression approach) normalized to CI chondrite Ivuna (Wang et al., 2015). Elements are arranged according to decreasing siderophility during lunar core formation from left to right (Steenstra et al., 2017; Wood et al., 2014). Previous estimates for the lunar mantle (Bombardieri et al., 2005; Chen et al., 2015; Ding et al., 2018; Hauri et al., 2015; Ni et al., 2019; O'Neill, 1991; Righter, 2019) and the model composition of the bulk silicate Earth (Wang and Becker, 2013, 2015) are shown for comparison.

used to estimate the mass fractions of SVE in the mantle source (e.g., Righter, 2019). Comparison of both methods shows that inverse modeling of 10% partial melting of the Apollo 12 olivine basalt source and 15% partial melting of the Apollo 15 olivine-normative basalt source yield mass fractions similar to the regression of SVE/RLE ratios for each basalt suite (Table 2). Calculated mass fractions are generally low, but reveal discernible differences between the mantle sources of the Apollo 15 and Apollo 12 low-Ti mare basalts. In contrast, almost identical and very low mass fractions are calculated for Cd. However, the Cd inventory is most likely affected by magmatic degassing (see discussion above) and the calculated mantle source values need to be considered as minimum values.

The modeled source compositions are strongly fractionated (Fig. 6) with different element ratios between the Apollo 15 (Cu/Ag ~~1~~0.000-13.000, C/S ~~0~~.014-0.015) and the Apollo 12 (Cu/Ag 6600-8200, Cu/S = 0.009-0.010) mantle sources. The strongest fractionations of the SVE inventory of mare basalts are expected for residual sulfide or metal in the mantle sources after melting. According to recent experimentally determined sulfur concentrations at sulfide saturation in low-Ti mare basalt compositions (1800-3500 µg/g, Ding et al., 2018), sulfides in lunar mantle sources should have been exhausted within the first 2-3% of partial melting. In contrast, other studies suggest that at the presumed reduced conditions of the mare basalt source regions, primitive mare basalts could be saturated in a S-poor, Fe-rich sulfide melt during melting (e.g., Brenan et al., 2019). At present, available data are insufficient to distinguish between these different models. If we accept the notion that most lunar mantle-derived basalts were sulfide-undersaturated after segregation from their sources, fractionations between mantle source and melt can only occur for SVE with sufficiently high partition coefficients for residual silicate phases. Recently Li et al. (2022) demonstrated that mantle silicates can host up to 20% of the mantle inventory of Cu, suggesting that the Cu/Ag ratio of mantle melts could deviate by up to 50% from the initial mantle value. However, in order to explain the difference in Cu/Ag ratios between different low-Ti mare basalt sources three times higher mass fractions and four times higher degree of partial melting would be required for Apollo 15 mare basalts. This would be inconsistent with the similar major element composition and almost identical RLE ratios (e.g., Ba/Sm = 14-17) of low-Ti mare basalts suites. Therefore, the observed differences between low-Ti mare basalt suites cannot be explained by magmatic fractionation processes, but point to discernible differences in mantle source compositions.

Our estimated mass fractions of S in the low-Ti mare basalt mantle sources are similar to previous bulk lunar mantle estimates of 70-80 µg/g (Fig. 6). In contrast mass fractions of Cu and Ag in our model composition are lower than many previous results inferred from Cu/Ti, Cu/Mn, and Ag/U ratios; at least partly this reflects analytical difficulties in some prior studies. In this regard high-quality isotope dilution ICP-MS data show their great potential to disentangle fractionation processes and source compositions. High-Ti mare basalts evolve from different source compositions and have a more complex magmatic history (Neal et al., 1990). The current data do not permit to estimate reliable SVE abundances in high-Ti mare basalt mantle sources.

4.3.2. Core formation, volatile loss and late accretion

The estimated mantle source compositions of low-Ti mare basalts reveal variable depletions of SVE when compared to the model composition of the BSE (Fig. 6). In the terrestrial mantle, the inventories of Cu, S, and Se are mainly governed by high P-T core formation and late accretion which contributed mainly to the abundances of S, Se and Te (Rose-Weston et al., 2009; Wang and Becker, 2013, 2015). At the relatively low P-T conditions during lunar core formation, Cu is more siderophile (Wood et al., 2014) whereas S and Se are less siderophile (Steenstra et al., 2017) compared to high P-T conditions that are relevant for Earth (Rose-Weston et al., 2009). Therefore, we argue that the estimated low Cu concentrations of the mantle sources of mare basalts and magnesian suite rocks and their moderately suprachondritic Cu/S and Cu/Se ratios predominantly reflect lunar core formation and not volatilization processes. In contrast, the strongly suprachondritic Cu/Ag ratios cannot be explained by lunar core formation, because at these conditions both elements strongly partition into metal (D_{Cu}/D_{Ag} 0.6-1.8 for 0-36 wt.% S in the metal melt; Wood et al., 2014). The upper limit of Cu/Ag in the low-Ti mantle source (~13.000) is almost four times higher than the BSE estimate of 3500 (Wang and Becker, 2015) and more than ten times higher than Cu/Ag in CI chondrites (Wang et al., 2015). Since Ag is significantly more volatile than Cu during nebular condensation (Wood et al., 2019) and during degassing from reduced mafic melts (Norris and Wood, 2017), volatility-controlled losses of Ag are the most plausible causes of the high Cu/Ag of lunar mantle sources. Because the differences in Cu/Ag ratios between different mare basalt suites (Fig. 5b) cannot have been caused by magmatic processes (see discussion above), they likely indicate differences in their mantle source compositions established by variable degrees of degassing during the LMO stage or earlier.

Based on HSE abundances and broadly chondritic $^{187}Os/^{188}Os$ of lunar mare basalts, Day and Walker (2015) estimated late accretion of 0.02% of the lunar mass to the mantle, more than 1000 times less material than accreted late to Earth. Assuming a similar SVE composition of lunar late accreted material as proposed for Earth (i.e., CM chondrite like, Wang and Becker, 2013), less than 3% of Cu, 10% S, 20% Se, and 40% Ag of the lunar mantle inventory might have been added late. Considering the uncertainties involved, we conclude that late accretion most likely contributed only minor fractions to the inventory of SVE in the lunar mantle, except for elements (Ag, Te, In, Cd, Tl) which were strongly depleted by volatile loss.

5. Summary and conclusion

In order to better constrain the SVE inventory of pristine highland rocks and mare basalts and to better understand the effects of volatile loss at different stages of the lunar magmatic evolution we determined mass fractions of SVE by isotope dilution ICP-MS. Consistent with RNAA data, the concentrations of most SVE in lunar magmatic rocks are low. Contrary to earlier data, we find correlations with indicators of fractional crystallization for Cu, S, Se, and Ag in mare basalts. Combined with similar mass fractions and element ratios in plutonic magnesian suite rocks we conclude that mass fractions of these elements in lunar igneous rocks are dominantly controlled by fractional crystallization and much less by late-stage magmatic degassing. The recent model of a volatile-rich lunar interior depends on the assumption of substantial magmatic degassing of many elements from lunar mantle melts (e.g., Chen et al., 2015; Hauri et al., 2015). Our data do not lend support to this hypothesis. In contrast, new estimates for the composition of the mantle sources of low-Ti mare basalt suites reveal low mass fractions of Cu, Ag, S, and Se, but also element ratios significantly distinct from BSE. These results suggest that the concentrations of Cu, S, and Se in the mantle sources dominantly reflect the conditions during lunar core formation. In contrast, the high Cu/Ag ratio cannot be explained by metal-sulfide-silicate partitioning and is the result of large-scale loss of Ag and presumably also other SVE such as Te, Cd, In and Tl prior to the formation of the man- tle sources. Together these results show that SVE can be sensitive tracers for volatile loss prior to the solidification of mantle source regions. Furthermore, the results support a lunar mantle which is heterogeneous and more depleted in SVE than the BSE and contains a lower fraction of late accreted material than Earth's mantle. Some more volatile elements (Cd, In, Tl) show disturbed frac- tional crystallization trends in mare basalts which indicates par- tial degassing of these elements from the cooling magmas and/or post-crystallization redistribution. The enrichment of more volatile SVE in brecciated anorthosites differ from observations for magne- sian suite clasts in impact melt breccia boulders. These differences suggest condensation of SVE from different gas compositions either due to a different origin or different temperatures of the gas phases.

CRediT authorship contribution statement

Philipp Gleißner: Conceptualization, Investigation, Visualization, Writing – original draft, Writing – review & editing. **Julie Salme:** Investigation, Writing – original draft. **Harry Becker:** Conceptualization, Supervision, Writing – original draft, Writing – review & editing.

Declaration of competing interest

The authors declare that they have no known competing financial interests or personal relationships that could have appeared to influence the work reported in this paper.

Acknowledgements

The authors wish to thank CAPTEM and the Lunar Sample Curator and his team for sample allocation. We thank S. Klemme for discussion, C. Renggli and J. Brenan for constructive reviews, which helped to improve the manuscript, and R. Dasgupta for editorial handling. Funded by the Deutsche Forschungsgemeinschaft (DFG, German Research Foundation) – Project-ID 263649064 – TRR 170. JS was funded by a TRR 170 fellowship. This is TRR 170 Publication No. 161.

Appendix A. Supplementary material

Supplementary material related to this article can be found online at https://doi.org/10.1016/j.epsl.2022.117680.

References

Albarède, F., Albalat, E., Lee, C.T.A., 2015. An intrinsic volatility scale relevant to the Earth and Moon and the status of water in the Moon. Meteorit. Planet. Sci. 50, 568–577.

Bombardieri, D.J., Norman, M.D., Kamenetsky, V.S., Danyushevsky, L.V., 2005. Major element and primary sulfur concentrations in Apollo 12 mare basalts: the view from melt inclusions. Meteorit. Planet. Sci. 40, 679–693.

Brenan, J.M., Mungall, J.E., Bennett, N.R., 2019. Abundance of highly siderophile elements in lunar basalts controlled by iron sulfide melt. Nat. Geosci. 12, 701–706.

Chen, Y., Zhang, Y., Liu, Y., Guan, Y., Eiler, J., Stolper, E.M., 2015. Water, fluorine, and sulfur concentrations in the lunar mantle. Earth Planet. Sci. Lett. 427, 37–46.

Day, J.M., Paquet, M., 2021. Temporally limited late accretion after core formation in the Moon. Meteorit. Planet. Sci. 56 (4), 683–699.

Day, J.M.D., 2018. Geochemical constraints on residual metal and sulfide in the sources of lunar mare basalts. Am. Mineral. 103, 1734–1740.

Day, J.M.D., Sossi, P.A., Shearer, C.K., Moynier, F., 2019. Volatile distributions in and on the Moon revealed by Cu and Fe isotopes in the 'Rusty Rock' 66095. Geochim. Cosmochim. Acta 266, 131–143.

Day, J.M.D., van Kooten, E.M., Hofmann, B.A., Moynier, F., 2020. Mare basalt meteorites, magnesian-suite rocks and KREEP reveal loss of zinc during and after lunar formation. Earth Planet. Sci. Lett. 531, 115998.

Day, J.M.D., Walker, R.J., 2015. Highly siderophile element depletion in the Moon. Earth Planet. Sci. Lett. 423, 114–124.

Day, J.M.D., Walker, R.J., James, O.B., Puchtel, I.S., 2010. Osmium isotope and highly siderophile element systematics of the lunar crust. Earth Planet. Sci. Lett. 289, 595–605.

Ding, S., Hough, T., Dasgupta, R., 2018. New high pressure experiments on sulfide saturation of high-FeO* basalts with variable TiO_2 contents – implications for the sulfur inventory of the lunar interior. Geochim. Cosmochim. Acta 222, 319–339.

Dygert, N., Liang, Y., Hess, P., 2013. The importance of melt TiO_2 in affecting major and trace element partitioning between Fe–Ti oxides and lunar picritic glass melts. Geochim. Cosmochim. Acta 106, 134–151.

Elkins-Tanton, L.T., Burgess, S., Yin, Q.-Z., 2011. The lunar magma ocean: reconciling the solidification process with lunar petrology and geochronology. Earth Planet. Sci. Lett. 304, 326–336.

Floss, C., James, O.B., McGee, J.J., Crozaz, G., 1998. Lunar ferroan anorthosite petrogenesis: clues from trace element distributions in FAN subgroups. Geochim. Cosmochim. Acta 62, 1255–1283.

Goldberg, R., Tombrello, T., Burnett, D., 1976. Fluorine as a constituent in lunar magmatic gases. In: Lunar and Planetary Science Conference Proceedings, pp. 1597–1613.

Hallis, L., Anand, M., Strekopytov, S., 2014. Trace-element modelling of mare basalt parental melts: implications for a heterogeneous lunar mantle. Geochim. Cosmochim. Acta 134, 289–316.

Hauri, E.H., Saal, A.E., Rutherford, M.J., Van Orman, J.A., 2015. Water in the Moon's interior: truth and consequences. Earth Planet. Sci. Lett. 409, 252–264.

Kato, C., Moynier, F., Valdes, M.C., Dhaliwal, J.K., Day, J.M., 2015. Extensive volatile loss during formation and differentiation of the Moon. Nat. Commun. 6, 7617.

Krähenbühl, U., Ganapathy, R., Morgan, J.W., Anders, E., 1973. Volatile elements in Apollo 16 samples: implications for highland volcanism and accretion history of the moon. In: Proceedings, 4th Lunar and Planetary Science Conference, pp. 1325–1348.

Li, Y., Li, Y-X., Xu, Z., 2022. The partitioning of Cu and Ag between minerals and silicate melts during partial melting of planetary silicate mantles. Geochim. Cosmochim. Acta 324, 280–311.

McCubbin, F.M., Kaaden, K.E.V., Tartèse, R., Klima, R.L., Liu, Y., Mortimer, J., Barnes, J.J., Shearer, C.K., Treiman, A.H., Lawrence, D.J., 2015. Magmatic volatiles (H, C, N, F, S, Cl) in the lunar mantle, crust, and regolith: abundances, distributions, processes, and reservoirs. Am. Mineral. 100, 1668–1707.

Meyer, C., 2010. Lunar sample compendium. In: Lunar and Planetary Science Conference. Abstract #1016.

Neal, C.R., Taylor, L.A., Hughes, S.S., Schmitt, R.A., 1990. The significance of fractional crystallization in the petrogenesis of Apollo 17 Type A and B high-Ti basalts. Geochim. Cosmochim. Acta 54, 1817–1833.

Ni, P., Zhang, Y., Chen, S., Gagnon, J., 2019. A melt inclusion study on volatile abundances in the lunar mantle. Geochim. Cosmochim. Acta 249, 17–41.

Norris, C.A., Wood, B.J., 2017. Earth's volatile contents established by melting and vaporization. Nature 549, 507.

O'Neill, H.S.C., 1991. The origin of the Moon and the early history of the Earth—A chemical model. Part 1: the Moon. Geochim. Cosmochim. Acta 55, 1135–1157.

Paniello, R.C., Day, J.M., Moynier, F., 2012. Zinc isotopic evidence for the origin of the Moon. Nature 490, 376.

Puchtel, I., Touboul, M., Blichert-Toft, J., Walker, R., Brandon, A., Nicklas, R., Kulikov, V., Samsonov, A., 2016. Lithophile and siderophile element systematics of Earth's mantle at the Archean–Proterozoic boundary: evidence from 2.4 Ga komatiites. Geochim. Cosmochim. Acta 180, 227–255.

Renggli, C.J., Klemme, S., 2021. Experimental investigation of Apollo 16 "Rusty Rock" alteration by a lunar fumarolic gas. J. Geophys. Res., Planets 126, e2020JE006609.

Rhodes, J., Blanchard, D., Dungan, M., Brannon, J., Rodgers, K., 1977. Chemistry of Apollo 12 mare basalts-Magma types and fractionation processes. In: Lunar and Planetary Science Conference Proceedings, pp. 1305–1338.

Righter, K., 2019. Volatile element depletion of the Moon—the roles of precursors, post-impact disk dynamics, and core formation. Sci. Adv. 5, eaau7658.

Rose-Weston, L., Brenan, J.M., Fei, Y.W., Secco, R.A., Frost, D.J., 2009. Effect of pressure, temperature, and oxygen fugacity on the metal-silicate partitioning of Te, Se, and S: Implications for Earth differentiation. Geochim. Cosmochim. Acta 73, 4598–4615.

Ryder, G., Schuraytz, B.C., 2001. Chemical variation of the large Apollo 15 olivine-normative mare basalt rock samples. J. Geophys. Res., Planets 106, 1435–1451.

Saal, A.E., Hauri, E.H., 2021. Large sulfur isotope fractionation in lunar volcanic glasses reveals the magmatic differentiation and degassing of the Moon. Sci. Adv. 7, eabe4641.

Shearer, C.K., Elardo, S.M., Petro, N.E., Borg, L.E., McCubbin, F.M., 2015. Origin of the lunar highlands Mg-suite: an integrated petrology, geochemistry, chronology, and remote sensing perspective. Am. Mineral. 100, 294–325.

Shearer, C.K., Hess, P.C., Wieczorek, M.A., Pritchard, M.E., Parmentier, E.M., Borg, L.E., Longhi, J., Elkins-Tanton, L.T., Neal, C.R., Antonenko, I., 2006. Thermal and magmatic evolution of the Moon. Rev. Mineral. Geochem. 60, 365–518.

Snape, J.F., Nemchin, A.A., Whitehouse, M.J., Merle, R.E., Hopkinson, T., Anand, M., 2019. The timing of basaltic volcanism at the Apollo landing sites. Geochim. Cosmochim. Acta 266, 29–53.

Steenstra, E., Lin, Y., Dankers, D., Rai, N., Berndt, J., Matveev, S., Westrenen, W., 2017. The lunar core can be a major reservoir for volatile elements S, Se, Te and Sb. Sci. Rep. 7, 1–8.

Walker, D., Longhi, J., Kirkpatrick, R.J., Hays, J.F., 1976. Differentiation of an Apollo 12 picrite magma. In: Lunar and Planetary Science Conference Proceedings, pp. 1365–1389.

Wang, K., Jacobsen, S.B., 2016. Potassium isotopic evidence for a high-energy giant impact origin of the Moon. Nature 538, 487–490.

Wang, Z.C., Becker, H., 2013. Ratios of S, Se and Te in the silicate Earth require a volatile-rich late veneer. Nature 499, 328–332.

Wang, Z.C., Becker, H., 2015. Abundances of Ag and Cu in mantle peridotites and the implications for the behavior of chalcophile elements in the mantle. Geochim. Cosmochim. Acta 160, 209–226.

Wang, Z.C., Becker, H., 2017. Chalcophile elements in Martian meteorites indicate low sulfur content in the Martian interior and a volatile element-depleted late veneer. Earth Planet. Sci. Lett. 463, 56–68.

Wang, Z.C., Becker, H., Wombacher, F., 2015. Mass Fractions of S, Cu, Se, Mo, Ag, Cd, In, Te, Ba, Sm, W, Tl and Bi in geological reference materials and selected carbonaceous chondrites determined by isotope dilution ICP-MS. Geostand. Geoanal. Res. 39, 185–208.

Warren, P.H., 1993. A concise compilation of petrologic information on possibly pristine nonmare Moon rocks. Am. Mineral. 78, 360–376.

Wing, B.A., Farquhar, J., 2015. Sulfur isotope homogeneity of lunar mare basalts. Geochim. Cosmochim. Acta 170, 266–280.

Wolf, R., Woodrow, A., Anders, E., 1979. Lunar basalts and pristine highland rocks-comparison of siderophile and volatile elements. In: Lunar and Planetary Science Conference Proceedings, pp. 2107–2130.

Wood, B.J., Kiseeva, E.S., Mirolo, F.J., 2014. Accretion and core formation: the effects of sulfur on metal–silicate partition coefficients. Geochim. Cosmochim. Acta 145, 248–267.

Wood, B.J., Smythe, D.J., Harrison, T., 2019. The condensation temperatures of the elements: a reappraisal. Am. Mineral. 104, 844–856.

Zhang, Y., 2021. Magnitude of stable isotope fractionation in lunar basalts. In: Lunar and Planetary Science Conference. Abstract #2548.